Physics of Shuttlecocks

Ho Kai Lun, Derrick Teo Hao Ying and Wang Shaodian
Hwa Chong Institution
Singapore, Singapore
hokl374@gmail.com

Chan Aik Hui, Phil
Faculty of Science, Department of Physics
National University of Singapore
Singapore, Singapore
phycahp@nus.edu.sg

***Abstract* — Badminton has gradually become of a topic of interest throughout the scientific community ever since 1992 when badminton became an Olympic sport and shuttlers were able to compete internationally for a title. Throughout the world many researchers have conducted experiments on the different aspects of badminton.**

Our research focuses on the trajectory and flight of the shuttlecock, observing various aspects of the trajectory e.g, shape, range and maximum height. We mathematically modelled this trajectory, known as the Tartaglia trajectory, to predict the various characteristics of the trajectory. We then conducted experiments using high speed cameras and Tracker™ Software to successfully verify our model. We also compared our own model to an existing model, concluding that our model is significantly better at predicting the range of the trajectory. We thereby examined the assumptions used to derive our literature model. We then plotted several graphs based on our models to examine their implications such as the theoretical initial angle for maximum range.

I. Introduction

Interest in badminton throughout the scientific community has been increasing ever since 1992 when badminton became an Olympic sport.

The shuttlecock experiences much greater aerodynamic drag during its flight compared to other projectiles, greatly altering its flight path, especially at high speeds.

As observed by Shibata, Pakorn, Sivakorn (2010) [1], this aerodynamic drag comes from the large surface area of feathers on a shuttlecock. The low mass of the shuttlecock increases the significance of aerodynamic drag. This results in a Tartaglia trajectory at high speeds.

A. Purpose and Research Question

We intend to mathematically model the trajectories of the shuttlecock and verify our models by comparing them to our experimental data and models put forth by Cohen, Darbois Texier, Dupeux, Brunel, Quéré, Clanet (2013) [2]. By doing this, we can better understand the trajectory of a shuttlecock and predict its range and maximum height.

Due to the significance of the aerodynamic drag, we hypothesise that the trajectory of the shuttlecock can be described by gravitational field strength and aerodynamic drag.

II. Methodology

A. Mathematical Model

To predict the trajectory of the shuttlecock and the characteristics of range and maximum height, we mathematically modelled the trajectory of the shuttlecock for the cases of laminar and turbulent airflow around it.

In our equations we use U_0 as the Initial Velocity, U_∞ as the terminal velocity of the shuttlecock, θ_0 as the launch angle (Figure 3), $h_{\text{-}th}$ as the maximum height and x_{0th} as range.

The aerodynamic characteristics of the shuttlecock are described by $\mathcal{L}$, the Aerodynamic length, defined by Cohen et al's (2013) [2] model:

$$\mathcal{L} = \frac{m}{\frac{1}{2}\rho C_D \pi R^2} \tag{1}$$

B. Laminar Flow

For Laminar Flow, aerodynamic drag force

$F_D = \frac{1}{2}\rho C_D \pi R^2 U$, therefore, $\mathcal{L} = \frac{U_\infty}{g}$

Where U is velocity, m is mass of shuttlecock, g is gravitational acceleration, ρ is density of air, C_D is drag coefficient and R is radius of shuttlecock.

Equation of motion:

$$m\frac{dU}{dt} = -mg - \frac{1}{2}\rho C_D \pi R^2 U \tag{2}$$

$$\frac{dU}{dt} = -g - \frac{U}{\mathcal{L}} \tag{3}$$

Integrating (3), we obtained these expressions:

Y-velocity w.r.t. time

$$U_y = \frac{\mathcal{L}g + U_0 \cdot \sin\theta_0}{e^{t/\mathcal{L}}} - \mathcal{L}g \tag{4}$$

X-velocity w.r.t. time

$$U_x = U_0 \cdot \cos\theta_0 \cdot e^{-t/\mathcal{L}} \tag{5}$$

Y displacement with respect to X displacement

$$y = \frac{x \cdot (U_\infty + U_0 \cdot \sin\theta_0)}{U_0 \cdot \cos\theta_0} + \mathcal{L}^2 g \cdot \ln\left|1 - \frac{x}{\mathcal{L} \cdot U_0 \cos\theta_0}\right| \tag{6}$$

The y-velocity decreases rapidly at the start due to effects of both gravity and air resistance. After y-velocity reaches 0 m s^{-1} at maximum height, it increases slowly as shuttlecock accelerates downwards due to gravity. Air resistance keeps the acceleration low.

U_x decreases exponentially throughout the trajectory from $U_0 \cdot \cos\theta_0$ to 0 m s^{-1}.

C. *Turbulent Flow*

For turbulent flow, aerodynamic drag force

$F_D = \frac{1}{2}\rho C_D \pi R^2 U^2$, therefore, $\mathcal{L} = \frac{{U_\infty}^2}{g}$

Equation of motion:

$$m\frac{dU}{dt} = -mg - \frac{1}{2}\rho C_D \pi R^2 U^2 \quad (7)$$

$$\frac{dU}{dt} = -g - \frac{U^2}{\mathcal{L}} \quad (8)$$

Integrating (8), we obtained these expressions:

Y velocity w.r.t time

$$U_y = \sqrt{\mathcal{L}g} \cdot \tan\left(\tan^{-1}\left(\frac{U_0 \sin\theta_0}{\sqrt{\mathcal{L}g}}\right) - \sqrt{\frac{g}{\mathcal{L}}}t\right) \quad (9)$$

X velocity w.r.t. time

$$U_x = \frac{\mathcal{L} \cdot U_0 \cos\theta_0}{\mathcal{L} + tU_0 \cos\theta_0} \quad (10)$$

Y displacement w.r.t. X displacement

$$y = \mathcal{L} \ln \left| \frac{\cos\frac{1}{\mathcal{L}}\left(\mathcal{L}\tan^{-1}\left(\frac{U_0 \sin\theta_0}{\sqrt{\mathcal{L}g}}\right) - \sqrt{\mathcal{L}g}\,\frac{\mathcal{L}\left(e^{\frac{x}{\mathcal{L}}} - 1\right)}{U_0 \cdot \cos\theta_0}\right)}{\cos\tan^{-1}\left(\frac{U_0 \sin\theta_0}{\sqrt{\mathcal{L}g}}\right)} \right| \quad (11)$$

D. *Terminal velocity (U_∞)*

We conducted experiments with a shuttlecock to verify our mathematical models. The Victor Champion No.1 shuttlecock was used for our experiments.

To measure U_∞, we arranged our setup using a uniformly coloured wall and a 1 m length of measuring tape taped to the wall (Figure 1).

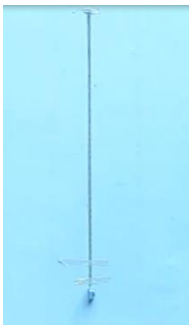

Figure 1. Set-up for Measurement of Terminal Velocity

Peastral, Lynch, Armenti (1980) suggested that shuttlecocks reach U_∞ after falling 9.2 m downwards [3]. We dropped our shuttlecock from a height of about 10 m above ground level. A high speed camera (Casio EX-ZR200) is set up in front of the wall slightly above ground level to film the bottom of the drop path at 300 frames per second (FPS).

The analysis is done by Tracker software by tracking the shuttlecock in the footage. Tracker is a software can determine the position of an object at a given instant, allowing us to calculate velocity by dividing the change in position of the shuttlecock by the time period.

E. *Experimental Setup for verification of models*

The experimental setup (Figure 2) was arranged in a school badminton hall to reduce the effect of wind on the trajectory of the shuttlecock. The table tennis table was used as the landing area due to its height being similar to the launch height of the shuttlecock, and this corresponds to our definition of x_{0th}. (Figure 3)

A 1.4 m measuring tape was placed on the table tennis table. We also sectioned the table horizontally in lengths of 20 cm to ensure more accurate measurement of x_{0th}.

The shuttlecock was launched by the shuttler, aiming for the Table Tennis table, with a badminton racquet. He was recorded with the Launcher Camera. The trajectory of the shuttlecock was recorded with the Trajectory Camera. Analysis of these footages using Tracker software allowed us to determine the variables θ_0, U_0, and h_{-th}. x_{0th} can be determined by adding the distance between shuttler and table with the reading on the measuring tape upon contact by the shuttlecock.

The Launcher Camera is a high speed camera set at 300 FPS and placed at close proximity to the shuttler. This ensures that the independent variables of our experiment, U_0 and θ_0, can be obtained with a high degree of accuracy.

The Trajectory Camera is a large aperture camera that was required to increase the brightness of the footage, due to the dark environment of the hall. Analysing this footage allowed us to determine h_{-th}.

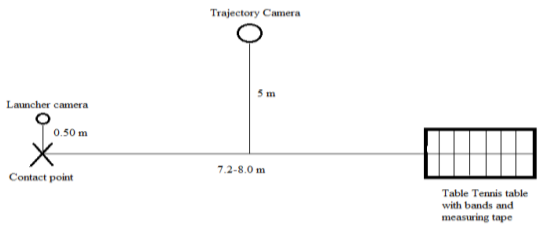

Figure 2. Experiment Setup (top view)

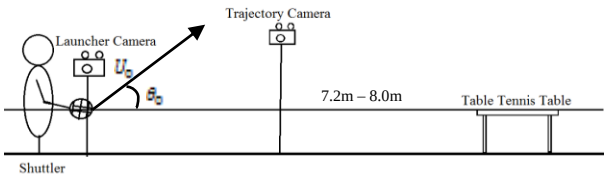

Figure 3. Experiment Setup (side view)

F. *Analysis*

We carried out our experiments and took sets of data points which each contain a value of θ_0 and U_0 (determined using Tracker software) and the corresponding x_{0th} and h_{-th} values.

In our analysis, we analysed and compared using Microsoft Excel the various results for each data set to our predicted results as well as those by the models of Cohen et al (2013) [2]. (Table II & III)

III. Results and Discussion

A. *Terminal Velocity*

The terminal velocity value measured (6.53 ± 0.53 m s^{-1}) was close to value of 6.7 m s^{-1} obtained by Cohen et al (2013) [2]. The turbulent flow C_D value ($2Mg/\rho U_\infty{}^2\pi R^2$) is 0.56, comparable to the value of 0.60 obtained by Cohen et al (2013) [2].

B. *Comparison of Models and Experimental Data*

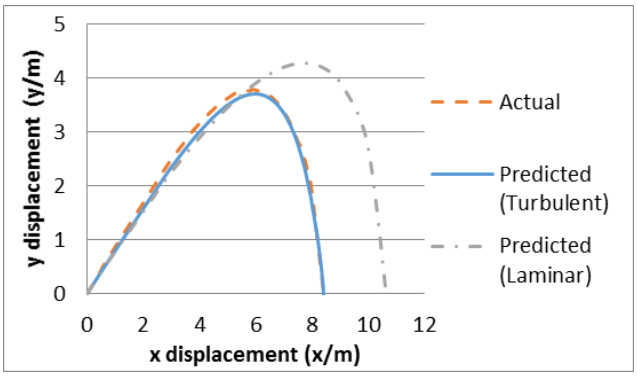

	Predicted (Turbulent)	Predicted (Laminar)
Root Mean Square Error (RMS)	0.116 m	0.997 m

Figure 4. Predicted Trajectories for Turbulent and Laminar flow compared with Actual Trajectory and Cohen et al's (2013) [2] predicted x_{0th}

The graph of experimental trajectory against predicted trajectories for turbulent and laminar flow were plotted on Microsoft Excel in Figure 4.

This graph shows that the airflow around the shuttlecock is most likely to be a turbulent rather than laminar flow, agreeing with present research [1]. The model that we proposed for turbulent flow also seems to fit extremely well with the experimental trajectory, compared to that for laminar flow, as shown by the much lower RMS values. Therefore, we would be using the turbulent flow model to derive expressions for x_{0th} and h_{-th} for comparison.

TABLE I. Comparison of x_{0th} and h_{-th} for predicted and experimental trajectories

	Range(x_{0th} / m)	Max Height h_{-th} /m
Predicted (Laminar)	10.8	4.28
Predicted (Turbulent)	8.40	3.71
Experimental	8.44	3.79

C. *Maximum Height*

Comparison

We derived an expression for the h_{-th} in the trajectory from equations 9-11:

$$h_{-th} = -\mathcal{L}\ln\left|\cos\tan^{-1}\left(\frac{U_0\sin\theta_0}{\sqrt{\mathcal{L}g}}\right)\right| \qquad (12)$$

This is compared with our data as well as Cohen et al's (2013) [2] model:

$$h_{-\text{th}} = \frac{1}{2}\mathcal{L}\sin\theta_0\ln\left[1+\left(\frac{U_0}{U_\infty}\right)^2\sin\theta_0\right]. \qquad (13)$$

TABLE II. Maximum height (h_{-th} / m) measurements for $\theta_0 = 42°$, $U_0 = 23.0$ m s^{-1}. The RMS values are for our full set of data.

θ_0/ °	U_0/m s^{-1}	h_{-th} /m
42.0	22.3	3.57
42.0	22.9	3.70
42.0	23.8	3.60
	Average	3.62 ± 0.06
Turbulent Predicted Value (42.0°, 23.0 m s^{-1})		4.09
Cohen et al 's Predicted Value (42.0°, 23.0 m s^{-1})		3.25
	Predicted (Turbulent)	Predicted(Cohen)
Root Mean Square	0.554 m	0.454 m

It can be seen in Table II that both our turbulent model as well as Cohen et al's (2013) [2] model for h_{-th} fit relatively well with our experimental data and her approximation of $h_{-th} \approx s_0 \sin\theta_0$ seems to hold well.

D. *Range*

Comparison

We also derived an expression for the x_{0th} based on our model in equation 11:

$$x_{0th} = \mathcal{L}\ln\left|U_0\cos\theta_0\sqrt{\frac{\mathcal{L}}{g}}\left\{\tan^{-1}\frac{U_0\sin\theta_0}{\sqrt{\mathcal{L}g}} + \tan^{-1}\sqrt{e^{\sqrt{\frac{\mathcal{L}}{g}}\ln\frac{\mathcal{L}g+(U_0\sin\theta_0)^2}{\mathcal{L}g}}-1}\right\}+\mathcal{L}\right| - \mathcal{L}\ln\mathcal{L} \qquad (14)$$

This is again compared with our empirical data as well as Cohen et al's (2013) [2] model:

$$x_{0\text{th}} = \frac{1}{2}\mathcal{L}\cos\theta_0\ln\left[1+4\left(\frac{U_0}{U_\infty}\right)^2\sin\theta_0\right] \qquad (15)$$

TABLE III. RANGE (x_{0th} / m) MEASUREMENTS FOR $\theta_0 = 42^o$, $U_0 = 23.0$ m s^{-1}. THE RMS VALUES ARE FOR OUR FULL SET OF DATA.

θ_0 / ^{o}	U_0 / m s^{-1}	x_{0th} / m
42.0	22.3	8.50
42.0	23.8	8.38
42.0	22.9	8.45
42.0	23.3	8.35
	Average	8.42 ± 0.07
Turbulent Predicted Value (42.0^o, 23.0 m s^{-1})		8.27
Cohen et al 's Predicted Value (42.0^o, 23.0 m s^{-1})		5.71
	Predicted (Turbulent)	Predicted (Cohen)
Root Mean Square (RMS)	0.369 m	2.71 m

This shows that our model for x_{0th} fits well with our experimental data. However, it can also be seen that Cohen et al's (2013) [2] model does not fit well with our data, giving a deviation of more than 2 m. (Table III)

Explanation for Deviation

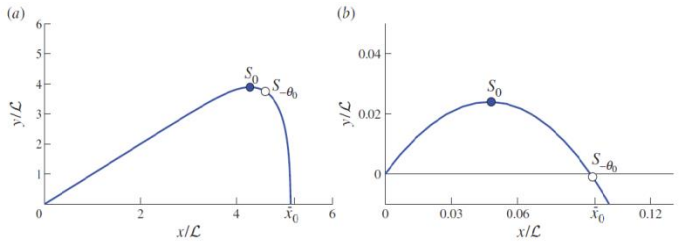

Figure 5. Arc distance ($s_{-\theta_0}$ / m) positions in Tartaglia (a) and Parabolic (b) Trajectory

Cohen et al (2013) [2] used the assumption of $x_0 = s_{-\theta 0} \cos\theta_0$ where $s_{-\theta 0}$ is the arc distance to the point where the instantaneous velocity angle is $-\theta_0$. This location is indicated by the white circle in both the Tartaglia and parabolic trajectories in Figure 5.

The Tartaglia curve is approximated as a right angle triangle where $s_{-\theta 0}$ represents the apex of the triangle. The parabolic curve is approximated as an isosceles triangle where $s_{-\theta 0}$ represents the intersection of the legs of the triangle.

Such an approximation is likely to hold well for extreme cases of the Tartaglia and parabolic curves but may not be suitable for a trajectory in between the 2 extremes.

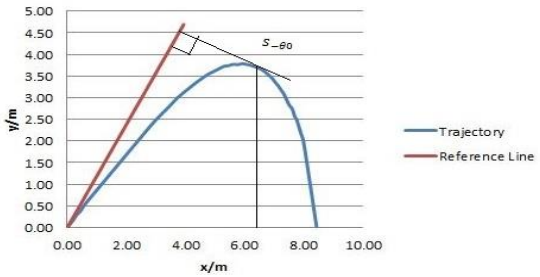

Figure 6. Arc distance ($s_{-\theta_0}$ / m) location in Transition Regime between Tartaglia and Parabolic Regime. Cohen et al's (2013) [2] predicted x_{0th} is around 6.5 m, while the x_{0th} was empirically found out to be above 8 m.

In Figure 6, an experimental trajectory is shown. The position of $s_{-\theta 0}$ is the intersection point between the line perpendicular to the reference line and the trajectory. The difference between the expected x_{0th} and experimental x_{0th} is about 2 m. This is close to the average difference between predicted and experimental x_{0th} shown in Table III.

E. Implications

As our turbulent flow model corresponds well with our experimental data, we now attempt to examine the implications of this model.

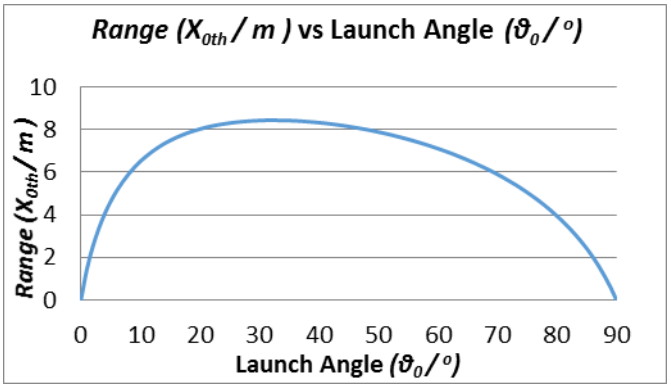

Figure 7. Plot of Range (x_{0th} / m) against Launch Angle (θ_0 / ^{o})

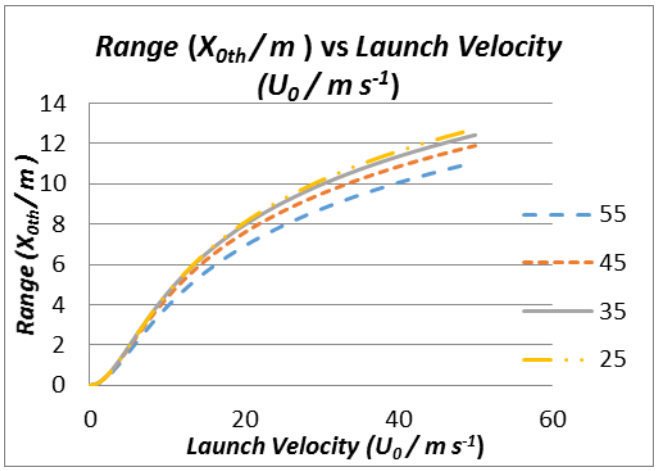

Figure 8. Plot of Range (x_{0th} / m) against Launch Velocity (U_0 / m s^{-1})

Predicted x_{0th} is plotted against θ_0 and U_0 in Figures 7 and 8. A horizontal asymptote is observed in the x_{0th} against U_0 graph at high U_0 values, an effect called the saturation of range that was also described by Cohen et al (2013) [2] in their model. At high U_0 values, x_{0th} remains relatively constant even when U_0 is increased by a large value.

The x_{0th} against θ_0 graph shows that the optimal launch angle to achieve maximum x_{0th} is about 32^o.

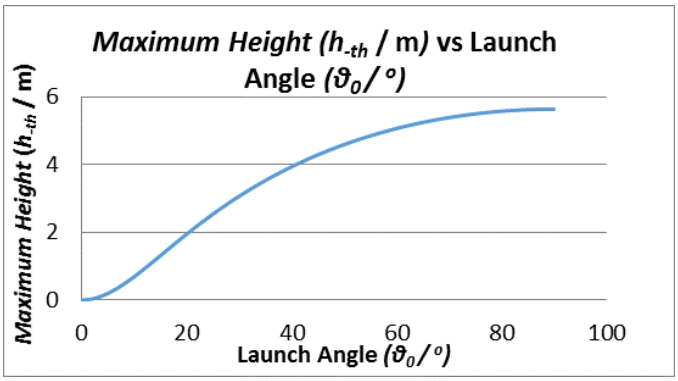

Figure 9. Plot of Maximum Height (h_{-th} / m) against Launch Angle (θ_0 /m s^{-1})

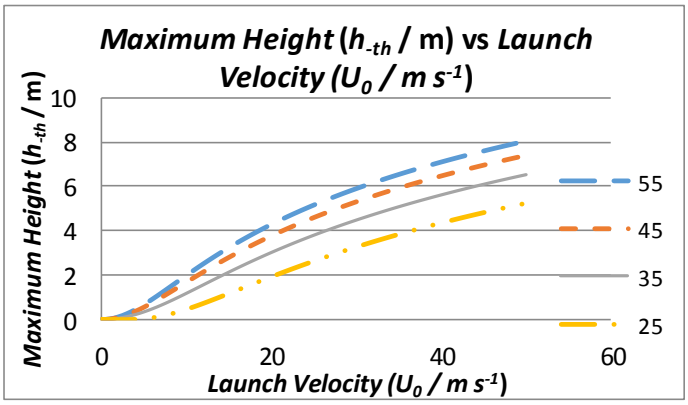

Figure 10. Plot of Maximum Height (h_{-th}/m) against Launch Velocity (U_0 /m s^{-1})

Predicted h_{-th} was also plotted against θ_0 and U_0 in Figures 9 and 10. It can be seen that h_{-th} is much more affected by U_0 than is x_{0th} at higher U_0 values.

The h_{-th} against θ_0 graph, as expected, indicates that the optimal launch angle to obtain h_{-th} is 90°.

IV. Conclusion

The mathematical model for turbulent airflow fits well with the experimental data we obtained, suggesting that the airflow around the shuttlecock is turbulent. Reynolds number obtained is about 2×10^5 at U_∞, generally accepted to suggest a turbulent airflow.

By comparing our data with models put forth by Cohen et al (2013) [2], her models do not seem to hold well in the experimental conditions that we used. Compared to the models by Cohen et al (2013) [2], our predictions for x_{0th} and h_{-th} are closer to the experimental values.

Measurements using different U_0 & θ_0 values

In order to verify the ln relationship between x_{0th} and U_0 in Figure 8, more experiments with values of U_0 < 20 m s^{-1} and U_0 > 40 m s^{-1} will need to be conducted.

More experiments with values of θ_0 < 35° and θ_0 > 50° will also need to be conducted to verify the predicted optimal angle for x_{0th} of 32° and that for h_{-th} of 90°.

Shuttlecock Launcher

One way we can improve the consistency of our experimental data is by building a shuttlecock launcher. This will helps us to consistently launch shuttlecocks at a specified launch velocity and angle.

One possible design would involve the compression of a spring in a tube. The shuttlecock is placed at the mouth of the tube. When the spring is released, it will launch a ball bearing towards the shuttlecock. When the ball bearing strikes the shuttlecock, it will transfer an impulse into the shuttlecock, launching it at a specific velocity and angle.

Flipping of Shuttlecock

Another area that we can study is the flipping of the shuttlecock. This area is an extremely interesting area to study due to the unique aerodynamic properties of the shuttlecock.

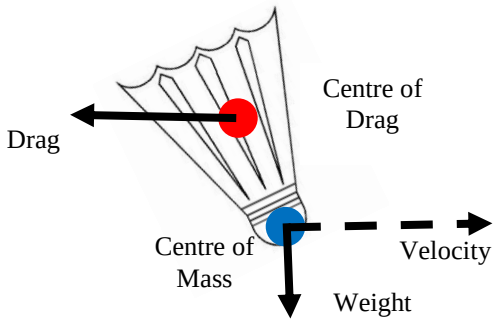

Figure 11. Vector Diagram for forces acting on shuttlecock during flight.

As seen in Figure 11 the Centre of Drag is in the feathers of the shuttlecock, since most of the drag a shuttlecock experiences is due to its feathers. [4]

However, the Centre of Mass is located in the base of the shuttlecock since that is where most of the mass of the shuttlecock is concentrated in.

The perpendicular distance between the Centre of Drag and Centre of Mass creates a moment on the shuttlecock, acting anti-clockwise in Figure 11. This means the shuttlecock will flip as the direction of drag changes at the top of the shuttlecock's trajectory.

V. References

[1] Shibata, M., Pakorn, A., & Sivakorn, S. (2010). Deceleration of the Shuttlecock. *ISB Journal of Physics*.

[2] Cohen, C., Baptiste, D.-T., Guillaume, D., Eric, B., David, Q., & Christopher, C. (30 September, 2013). The Aerodynamic Wall. *Proceedings of the Royal Society*, pp. 470 - 490.

[3] Peastrel, M., Lynch, R., & Armenti, Jr, A. (1980). Terminal Velocity of Shuttlecock in Vertical Fall. *American Journal of Physics*, 511 - 513.

[4] Baptiste Darbois Texiera, C. C. (2012). Shuttlecock Dynamics. *Procedia Engineering*, (pp. 176-181)